On the Mechanism of Martensite Formation during Short Fatigue Crack Propagation in Austenitic Stainless Steel: Experimental Identification and Modelling Concept

Ulrich Krupp[1,*], Ingmar Roth[2], Hans-Jürgen Christ[2], Martin Kübbeler[2], Claus-Peter Fritzen[2]

[1] Faculty of Engineering and Computer Science, University of Applied Sciences Osnabrück, 49009 Osnabrück, Germany
[2] Faculty IV: Science and Technology, University of Siegen, 57068 Siegen, Germany
* Corresponding author: u.krupp@hs-osnabrueck.de

Abstract During fatigue of metastable austenitic steels, local plasticity is linked with the formation of martensite. It was shown that cubic α´ martensite nucleates at slip band and ε martensite intersection sites ahead of growing fatigue cracks. Since such intersections require the operation of alternate slip systems, martensite formation was found only for shear-controlled single-slip crack propagation (mode II) prevailing during the early propagation phase of microstructurally short fatigue cracks. Surprisingly, cracks were found not to initiate within martensitically transformed grains but by a fraction of 70% along twin boundaries. The extent of martensite formation ahead of a propagating crack increases with increasing crack length and eventually, gives rise to transformation-induced crack-closure effects. The interaction between the crack tip plasticity and the local microstructure was quantitatively analysed by automated electron back-scatter diffraction (EBSD) in the scanning electron microscope (SEM) applied to the electro-polished surfaces of fatigue specimens. Following a geometrical model for martensitic transformation, further analysis of the relevant fatigue mechanism became possible aiming to both mechanism-based life prediction and tailoring fatigue resistant microstructures.

Keywords austenitic steels, martensitic transformation, fatigue crack propagation, short crack model

1. Introduction

Metastable austenitic stainless steels, e.g., AISI 304, may exhibit a transformation from fcc austenite into bcc martensite (α´ martensite) if a certain monotonic or cyclic plastic strain value is exceeded. This so-called TRIP effect (transformation-induced plasticity) is widely technically used, e.g., for work-hardened spring elements. From a thermodynamic point of view, at room temperature the Gibbs free energy difference ΔG between the fcc and the bcc phase is not large enough for spontaneous martensitic transformation to occur. However, this changes when sufficient plastic strain energy ΔG_{mech} is added, as it is schematically represented in Fig. 1a. Generally, the phase relationship between the parent fcc austenite and the martensite can be explained by the Bain relationship as shown in Fig. 1b [1]. From a microstructure point of view, plastic slip along the {111} slip planes of the fcc austenite cause the formation of extended stacking faults (due to the low stacking fault energy of the metastable austenitic steels), i.e., hexagonal ε martensite bands. The cubic α´ martensite nucleates at intersection points of the ε martensite bands (cf. [2,3]). Between the parent austenite and the transformed martensite, the Kurdjumov-Sachs relationship is fulfilled (cf. [4]):

$$\{111\}_{\gamma} \parallel \{101\}_{\alpha'} \quad \text{and} \quad <110>_{\gamma} \parallel <111>_{\alpha'} \quad . \tag{1}$$

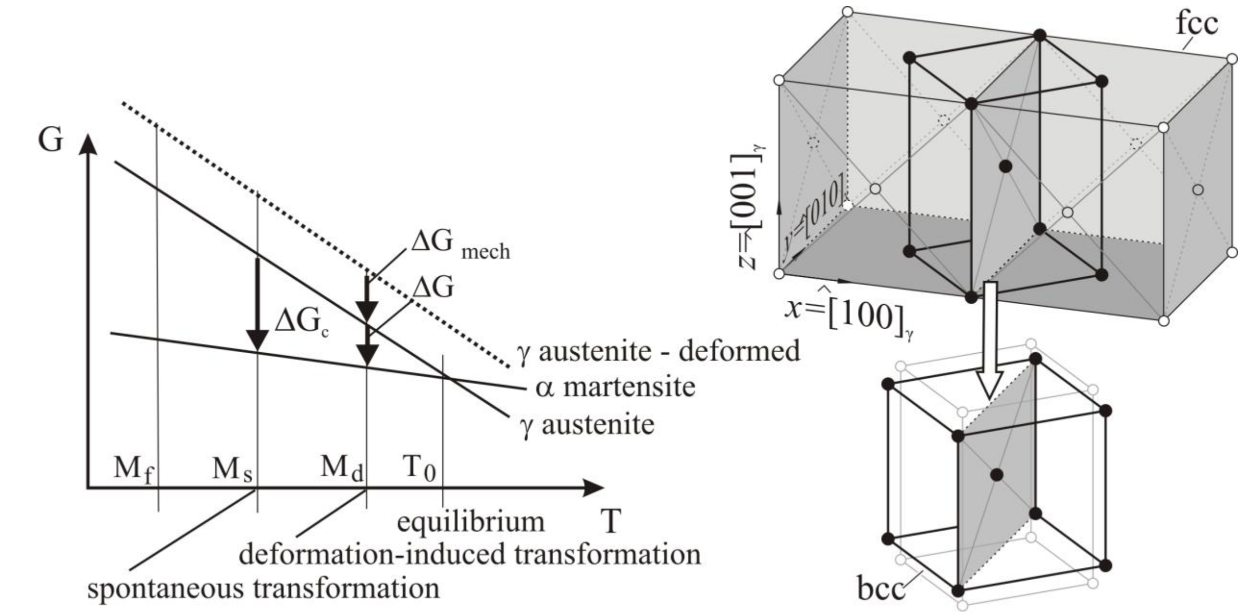

a b

Figure 1. (a) Contribution of the mechanical strain energy ΔG_{mech} to the thermodynamic driving force for austenite-to-martensite transformation and (b) unit cell model of the martensitic transformation, according to Bain [1].

According to Olson and Cohen [3], the α´ martensite volume fraction $f_{\alpha'}$ can be calculated as a function of the plastic strain ε_{pl} by Eq. 2:

$$f_{\alpha'} = 1 - \exp\left(-\beta\left(1-\exp\left(-\alpha\varepsilon_{pl}\right)\right)^n\right), \tag{2}$$

with n being a material-depending exponent, α a temperature-depending constant, and β accounting for the probability that martensite embryos are formed at shear-band intersections. While under monotonic loading conditions the α´ saturation level is reached at $f_\alpha \approx 0.9$, under cyclic loading conditions the transformation depends on the accumulative plastic strain $\varepsilon_{pl,\,cum}$ and sets in only when a critical threshold of $\Delta\varepsilon_{pl}/2 \approx 0.3$ is exceeded [5]. Under high-cycle fatigue (HCF) loading conditions and correspondingly very small $\Delta\varepsilon_{pl}$, plastic deformation is limited to grains of favorable orientation of the slip systems, with values of the Schmid factor $M_S \approx 0.5$. Smaga et al. [6] use the Olson-Cohen model to define a damage parameter that includes inhomogeneous cyclic hardening due to martensitic transformation. In very-high cycle fatigue (VHCF) Müller-Bollenhagen et al. [7] had shown that the onset of fatigue damage in form of local plasticity is stopped by martensite formation (self healing of defects); they concluded that metastable austenitic stainless steels exhibit a real fatigue limit. However, in the HCF regime short fatigue cracks may initiate without martensitic transformation. The propagation of such cracks cannot be shielded completely by the formation of martensite in the plastic zone ahead of the crack tip [4].

In order to understand and to predict the propagation behavior of microstructurally short fatigue cracks in metastable stainless steels, the geometrical model of Bogers and Burgers [8] was employed. It considers co-operative slip at two austenite slip systems as schematically represented in Fig. 2. Here, bcc α´ martensite nucleation is a product of partial dislocation displacement on every 2nd (T/2) and every 3rd (T/3) {111} slip plane, respectively.

$$\frac{T}{3} = \frac{1}{3}\cdot\frac{1}{6}a[211]_{fcc} \quad \text{and} \quad \frac{T}{2} = \frac{1}{2}\cdot\frac{1}{6}a[21\bar{1}]_{fcc} \quad . \tag{3}$$

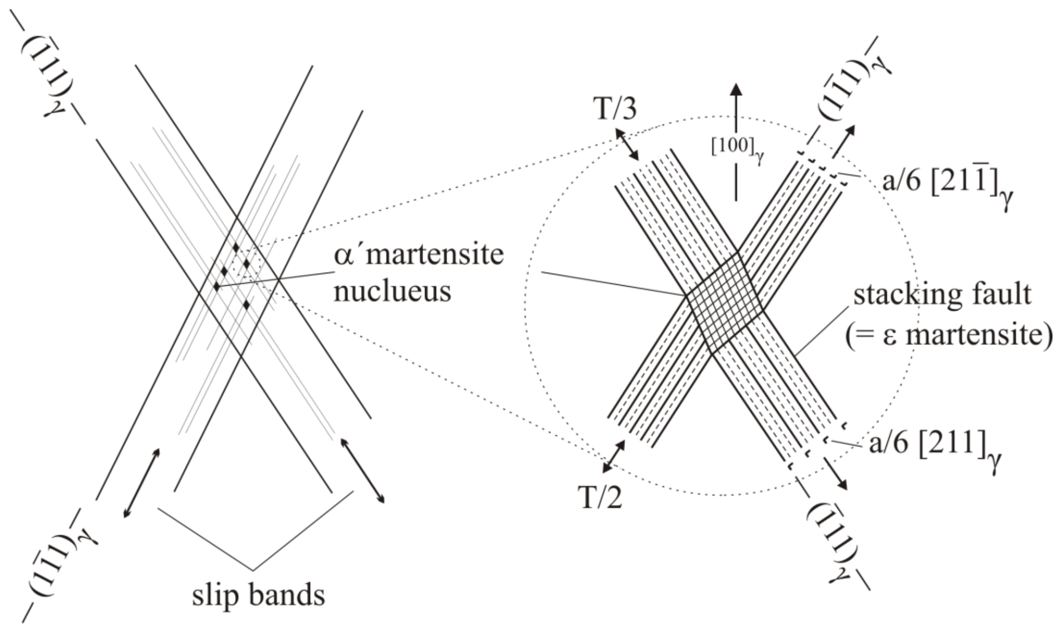

Figure 2. α´martensite nucleation at {111} slip-band intersection points, according to the model of Bogers and Burgers [8].

The Bogers-Burgers model for martensite formation at fcc shear band intersections has been proven experimentally in various studies and is the basis for the modeling concept introduced in section 4.

2. Experimental

The experiments were carried out on cylindrical specimens of the metastable austenitic stainless steel AISI 304L provided by Deutsche Edelstahlwerke Siegen, Germany, with the chemical composition given in Table 1. Prior fatigue testing, the specimen material was solution heat-treated for 1.5h at a temperature of 1050°C in order to homogenize the microstructure resulting in an average austenite grain size of 74µm. To analyze microstructurally short fatigue cracks within a limited area, two shallow notches were machined at 0° and 180° of the gauge length of the specimens (see Fig. 3). To apply electron channeling contrast (ECCI) and electron back-scatter diffraction (EBSD) within the scanning electron microscope (SEM), the surface of the specimens was electrolytically polished at T=-15°C/15V using perchloric acid (8%, cf. [9]).

Table 1. Chemical composition of the metastable austenitic steel used in this study (in wt. %).

alloy	Fe	C	Cr	Ni	Si	Mn	Cu	Mo
AISI 304L	Base	0.03	18.1	8.75	0.62	1.85	0.54	0.37

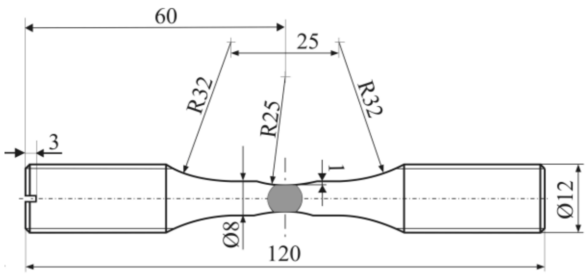

Figure 3. Shallow-notched specimens for microcrack characterization in a servohydraulic testing system.

Fatigue cracks were followed using a MTS810 servohydraulic testing system under load control at a stress ratio of R=-1. Crack length analyses and measurements of the crystallographic orientation/phase distributions were done in the SEM by periodically removing the specimens from the testing machine. The fatigue limit was estimated by rotating bending tests following the staircase approach.

3. Results

The fatigue limit of the AISI 304L test material was found to lie in the range between $\Delta\sigma/2$=230MPa and $\Delta\sigma/2$=240MPa. It is worth mentioning that (i) above a number of cycles of $N \approx 5 \cdot 10^5$ cycles no failure was observed at all and (ii) the fatigue limit is of the same order of magnitude than the 0.2%-offset yield strength of $R_{p0.2}$=237MPa. HCF microcrack propagation studies were carried out at a stress amplitude (fully reversed, R=-1) of $\Delta\sigma/2$=245MPa. After a few thousands of cycles, martensitic transformation occurred in favorable oriented grains of a high Schmid factor close to M_S=0.5. Furthermore, it is believed that the high elastic anisotropy of austenitic steel ($A=2C_{44}/(C_{11}-C_{12})=3.81$, cf. [10]) promotes the local transformation process, but obviously also crack initiation. About 70% of all crack initiation events (48 evaluated cracks) can be correlated with twin boundaries, which exhibit high anisotropy stresses, as it was analyzed in the studies of Heinz and Neumann [11] and Blochwitz and Tirschler [12]. Surprisingly, crack initiation cannot be correlated with martensitic transformation.

Figure 4a shows an example of crack initiation at a twin boundary. Only when the crack path leaves the twin boundary (above and below the twin boundary crack segment) and continues by alternating activation of various {111}<110>-type slip systems, martensite could be identified by means of EBSD phase analysis. Obviously, the slip intersections act as martensite nucleation sites, according to the theory of Olsen and Cohen [3] and Bogers and Burgers [8]. This observation is further supported by Fig. 4b. Again, the crack was initiated at a twin boundary segment. When following the right-hand branch of the crack, one may notice that propagation follows a {110} martensite plane. It is believed that the activation of alternate slip systems in the austenite ahead of the crack tip cause martensite formation. In the following, further crack propagation occurs within the martensite phase. In a more pronounced manner this was observed within the circle area in Fig. 2b. However, as long as fatigue crack propagation is driven by the activation of only one slip system, no martensite formation can be identified.

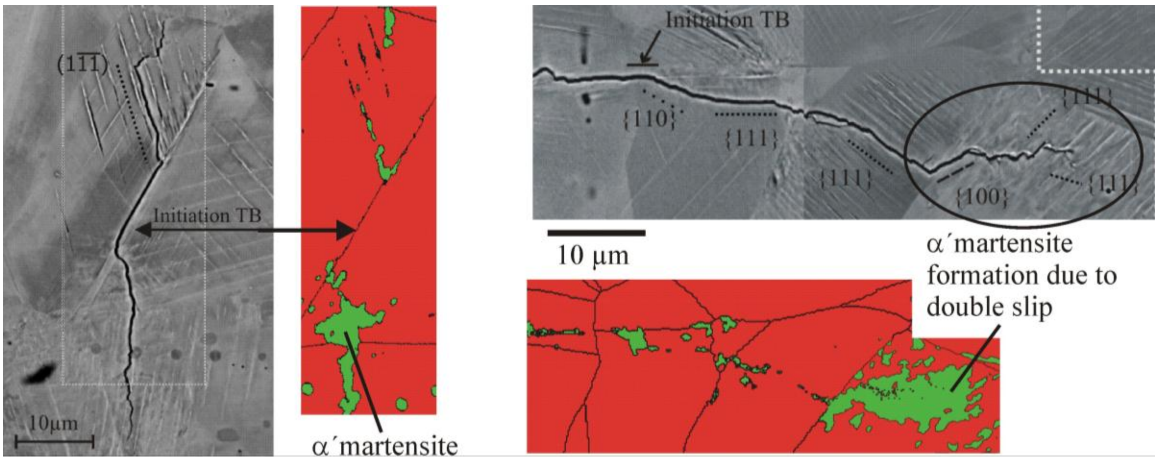

a b

Figure 4. Microstructurally short fatigue cracks: (a) crack initiation at a twin boundary without any martensite formation (see EBSD map beside) and (b) crack propagation operated by alternating slip in combination with massive martensite formation (see EBSD map below).

The Bogers-Burgers mechanism was identified by using transmission electron microscopy (TEM).

Figure 5 shows the intersection of {111} slip bands, which can be interpreted as stacking faults changing the stacking sequence from ABCABC with the fcc austenite to ABAB within the slip band. Such stacking faults correspond to ε martensite bands. Where these bands intersect bcc α´martensite is formed (see Fig. 5a).

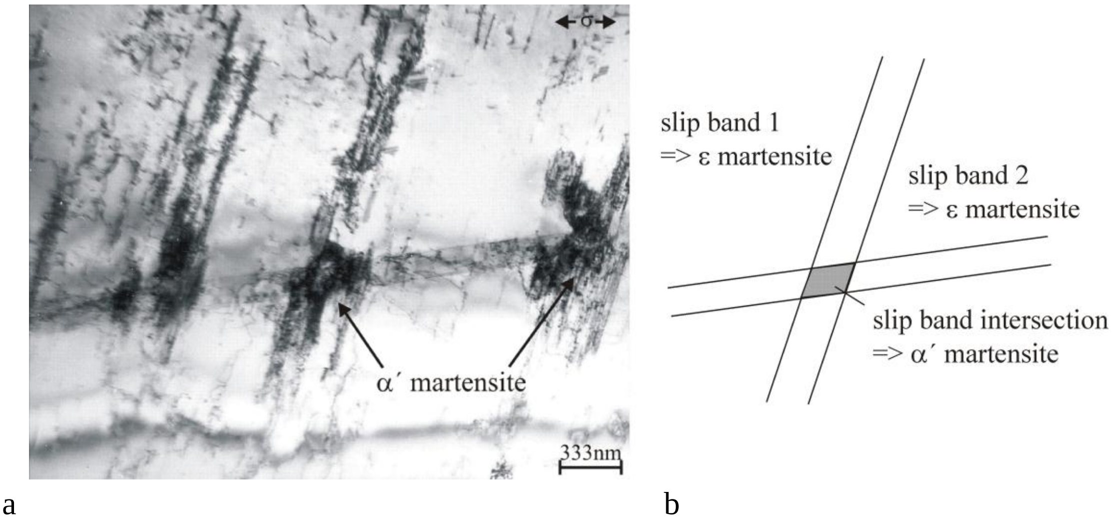

Figure 5. Deformation-induced α´ martensite formation during HCF loading of AISI 304L steel after N=10^5 cycles: (a) TEM micrograph and (b) schematic representation.

Analysis of the crack propagation rate as a function of the local microstructure revealed that the crack propagation rate decreases strongly, when (i) the propagation mode changes from single-slip propagation mode to double slip propagation mode, (ii) the crack propagates into transformation martensite, or when (iii) the crack tip approaches a grain boundary. Generally, the strong interactions between the plastic zone ahead of the crack tip and the local microstructural features give rise to an oscillating crack propagation rate, which was found at lower stress intensity ranges ΔK than the threshold value ΔK_{th}. The comparison of the propagation behavior of several microcracks with the one of a long crack is shown in Fig. 6.

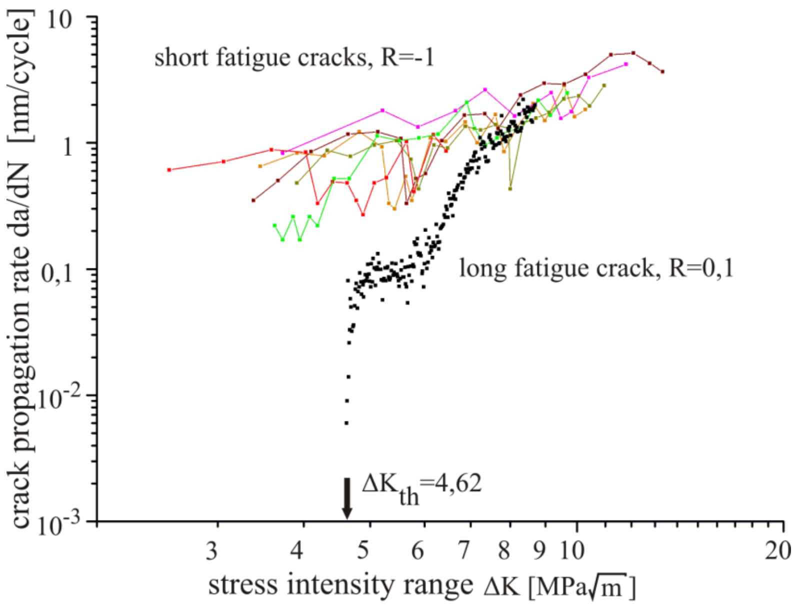

Figure 6. Propagation behavior of short (2a<400µm) and long fatigue cracks in metastable austenitic steel AISI 304L.

4. Modeling Concept and Discussion

It is the aim of the study to predict the complex propagation behavior of microstructurally short fatigue cracks, as presented in section 3. For this purpose a short crack model has been developed where the crack and its plastic zones are meshed by boundary elements (for details see [13,14]). The boundary elements represent shear displacements along individual slip planes and normal and shear displacements within the crack. Accounting for the boundary conditions that (i) within the crack the normal displacements must be positive and no shear stresses are present and (ii) the shear stress values within the slip bands are limited to the friction stress τ_{fr}, the equation system for the displacement distribution along crack and slip bands can be calculated. The crack propagation rate results from the cyclic crack tip slide displacement ΔCTSD as follows

$$\frac{da}{dN} = C \cdot \Delta CTSD, \tag{4}$$

where C represents the irreversible part of ΔCTSD that contributes to crack advance.
In order to account for the Bogers-Burgers mechanism of martensitic transformation (see section 1), the model has been extended to alternate slip ahead of the crack tip. Vector addition of the slip displacements b_{t1} and b_{t2} (see Fig. 7) give a resulting displacement b_R. The magnitude of these displacements determines the size of the corresponding martensitic transformation zone. The direction of the resulting displacement does not necessarily correspond to a slip direction of the martensite phase, the displacement b_R is projected onto the current crack propagation direction, eventually resulting in the crack tip displacement b_{RP} corresponding to CTSD within the crack propagation plane.

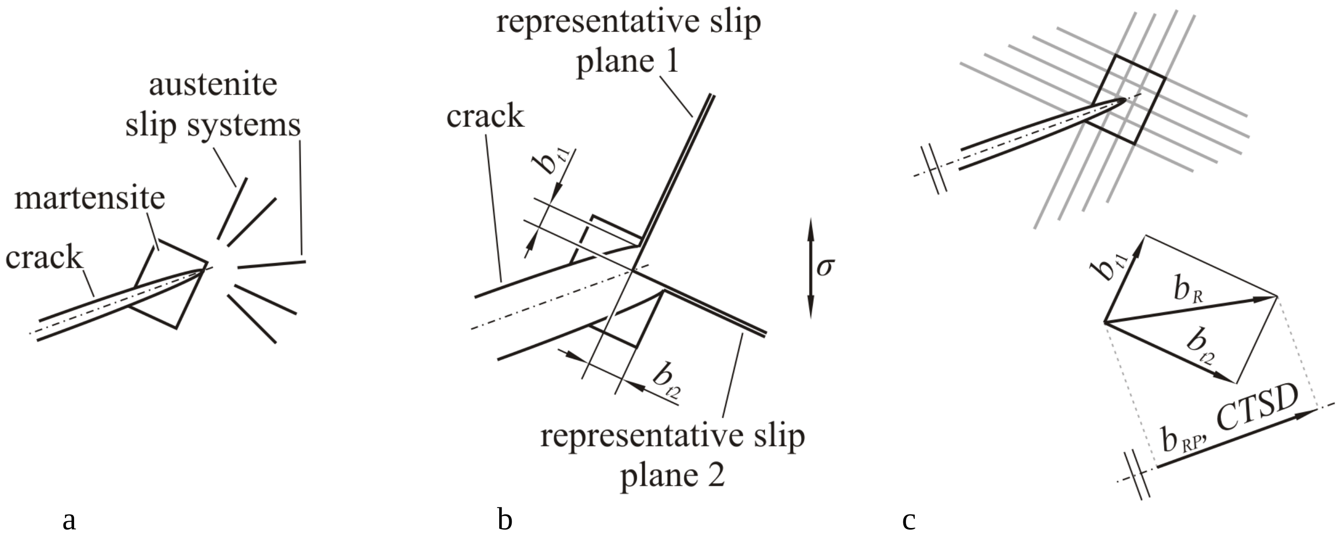

Figure 7. Modeling concept for strain-induced martensite formation ahead of a growing fatigue crack: (a) crack tip with martensite and the various austenite slip systems, (b) displacement at two representative slip planes, and (c) corresponding new martensite zone with the respective crack tip slide displacement.

As mentioned before, the austenite to martensite phase transformation results in a 2.57% volume increase. Therefore, a volume strain ε_m is implemented in the model. As schematically shown in Fig. 8, the martensite phase and the individual grain boundaries are meshed by boundary elements that describe absolute displacements of the boundaries. By superimposing the displacements within the plastic zone ahead of the crack tip (relative displacements) with those of the boundaries (accounting for the individual elastic properties) and the volume strain within the transformation zone, one can predict crack propagation.

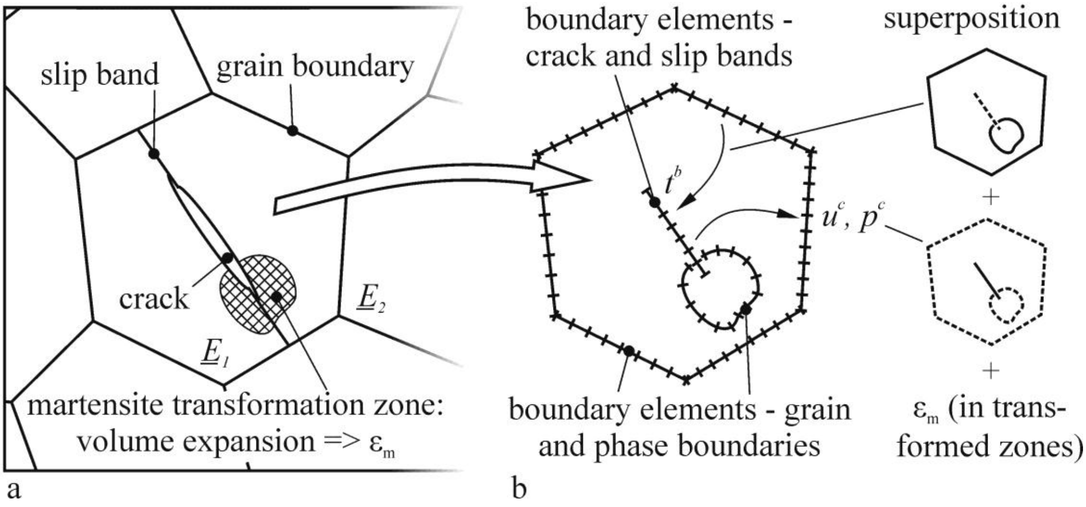

Figure 8: Schematic representation of the boundary element model: (a) crack with adjacent slip bands and martensite transformation zone in an individual grain of stiffness E_1 and (b) superimposition of crack-free grain, crack in an infinite plate and volume expansion strain ε_m.

Figure 9 shows the application of the model to a real microstructurally fatigue crack in AISI 304L. Certainly, the simulation shows a martensite distribution of much higher homogeneity than the experimental evaluation, but the predicted crack propagation rates are in reasonable agreement. Hence, one may conclude that the modeling concept represents the governing mechanisms in the right way, supporting the concept of Bogers and Burgers to be applicable to fatigue crack propagation in combination with martensitic transformation in metastable austenitic steels.

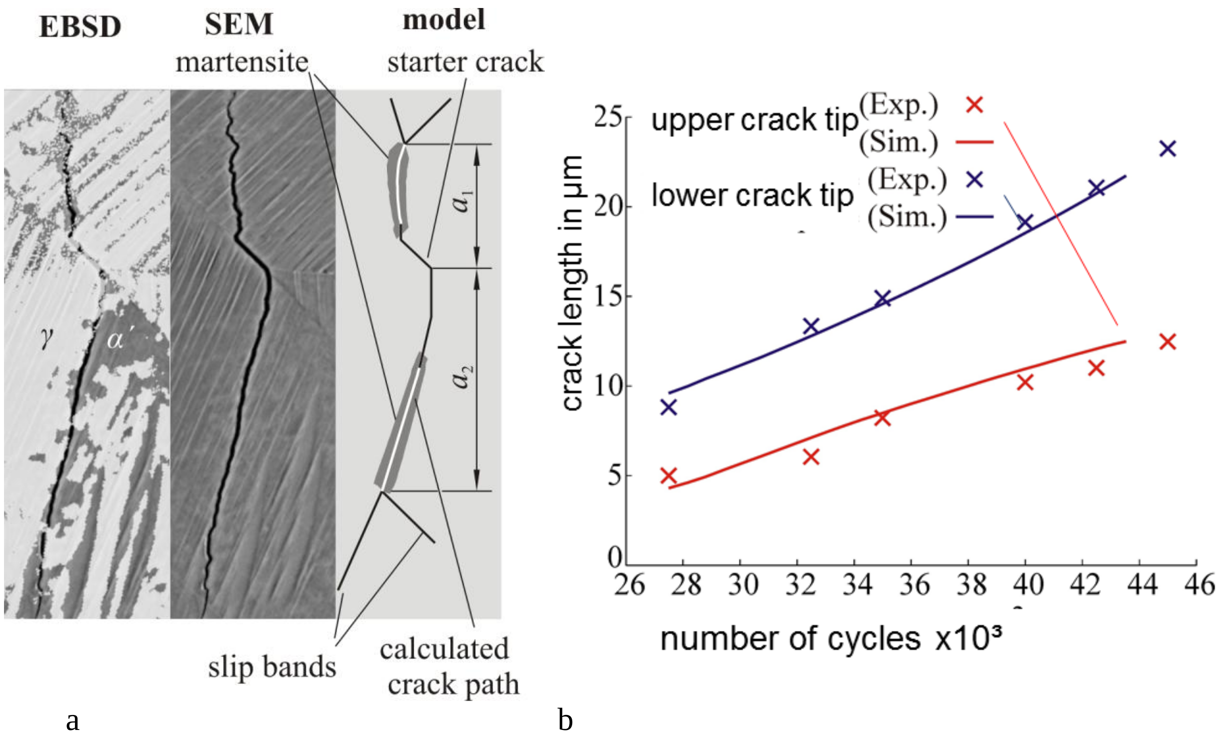

Figure 9. Microstructurally short fatigue crack in AISI 304L: (a) EBSD phase distribution, SEM micrograph and predicted strain induced martensite, (b) corresponding simulated vs. experimental fatigue crack propagation.

5. Conclusions

Crack propagation during high-cycle fatigue loading of metastable austenitic steel AISI 304L is not only governed by interactions with local microstructural features such as the alloy grain boundaries. Moreover, plastic slip ahead of the crack tip causes the formation of strain-induced α' martensite. According to a geometrical model of Bogers and Burgers, the fcc austenite to bcc martensite phase transformation can be described by co-operative activation of partial dislocations on two intersecting {111} type slip bands. It was proven by scanning and transmission electron microscopy that martensite formation occurs only within areas of multiple slip activation. For crack initiation and propagation along single slip bands no martensite formation was identified. Depending on the local crystallographic orientation of the grains with respect to the remote stress axis and depending an the amount of martensite phase formation, the crack propagation rate is increased or decreased, respectively. This can be qualitatively predicted by computer simulation using a boundary element approach where the crack and the possible slip planes are described by boundary elements allowing for martensitic transformation according to the Bogers-Burgers model.

Acknowledgements

The financial support by Deutsche Forschungsgemeinschaft DFG under grant no. PAK104 - KR1999/11 is gratefully acknowledged.

References

[1] E.C. Bain, The nature of martensite transformation, AIME Steel Division, 70 (1924) 25-46.

[2] H. Schumann, Bildung von α'-Martensit im Schnittbereich von ε-Martensitplatten, Kristall und Technik, 12 (1977) 363-370.

[3] G.B. Olsen, M. Cohen, Kinetics of strain-induced martensitic nucleation, Met. Mat. Trans, 6A (1975) 791-795.

[4] U. Krupp, I. Roth, H.-J. Christ, M. Kübbeler, C.-P. Fritzen: In-Situ SEM Observation and Analysis of Martensitic Transformation during Short Fatigue Crack Propagation in Metastable Austenitic Steel, Adv. Engng Mater., 12 (2010) 255.

[5] M. Bayerlein, H.-J., Christ, H. Mughrabi, Plasticity-induced martensitic transformation during cyclic deformation of AISI304L stainless steel, Mater. Sci. Engng A, 114 (1992) L11.

[6] M. Smaga, P. Starke, D. Eifler, J. Fingerhuth, B. Nieweg, D. Siegele, Bewertung der Ermüdungsfestigkeit metastabiler austenitischer Stähle unter Berücksichtigung zyklischer Ver- und Entfestigungsvorgänge, in: Fortschritte in der Werkstoffprüfung in Forschung und Praxis, M. Borutzki, G. Moninger (Eds.), Verlag Stahleisen, Düsseldorf, 2012, pp. 173-178.

[7] H.-J. Christ, C. Müller-Bollenhagen, M. Zimmermann, Effect of deformation induced martensite on the very high cycle fatigue properties of a metastable austenitic stainless steel, in: Proc. 5th Int. Conf. on Very High Cycle Fatigue (VHCF 5), C. Berger, H.-J. Christ (Eds.), DVM Berlin, 2011, pp. 171-176.

[8] A.J. Bogers, W.G. Burgers, Partial dislocations on the {110} planes in the bcc lattice and the transition of the fcc into the bcc lattice, Acta Metall. 12 (1964) 255-261.

[9] I. Roth, Untersuchungen zum Ausbreitungsverhalten mikrostrukturell kurzer Ermüdungsrisse in metastabilem austenitischen Edelstahl, doctorate thesis, University of Siegen, 2011.

[10] H.M. Ledbetter, Predicted monocrystal elastic constants of 304 type stainless steel, Physica 128B (1985) 1-4.

[11] A. Heinz, P. Neumann, Crack initiation during high-cycle fatigue of an austenitic steel, Acta Met. Mat. 38 (1990) 1933-1940.

[12] C. Blochwitz, W. Tirschler, Twin boundaries as crack nucleation sites, Cryst. Res. Techn. 40 (2005) 32-41.

[13] M. Kübbeler, I. Roth, U. Krupp, C.-P. Fritzen, H.-J. Christ: Simulation of Stage I-Crack Growth Using a Hybrid Boundary Element Technique, Engineering Fracture Mechanics, 78 (2011) 462.

[14] U. Krupp, Fatigue crack propagation in metals and alloys, Wiley VCH, Weinheim 2007.